

TOTAL REACTION CROSS-SECTION MEASUREMENTS WITH 60-MeV PROTONS*

J. J. H. Menet,† E. E. Gross, J. J. Malanify, and A. Zucker

Oak Ridge National Laboratory, Oak Ridge, Tennessee 37830

(Received 21 April 1969)

We have measured total reaction cross sections for 60-MeV protons on ^{12}C , ^{27}Al , ^{56}Fe , ^{58}Ni , ^{59}Co , ^{60}Ni , ^{68}Zn , ^{90}Zr , ^{120}Sn , and ^{208}Pb . We find that, contrary to previous measurements, our results agree with predictions of the optical model. For a fixed-geometry potential the volume absorption term is reasonably constant with A , while the surface absorption term increases monotonically from 0.12 MeV for Al to 4.2 MeV for Pb.

At the present time the optical model depends on three kinds of data: differential cross section and polarization for elastic scattering, and total reaction cross sections. It has recently become apparent that the optical model for protons was in serious trouble at energies higher than 40 MeV. In particular, the parameters required to fit elastic-scattering data¹ at 60 MeV predicted total reaction cross sections 30 to 40% higher than the measured values.² It was also noted¹ that parameters derived from proton elastic scattering agreed with the measured total reaction cross section at 55 MeV for neutrons³ but not for protons. We therefore concluded that either the optical model for protons above 40 MeV was breaking down or that the total reaction cross-section measurements were seriously in error. In any case, the situation was ripe for some critical experiments. We decided that the problem could be best resolved by measuring total reaction cross sections σ_R around 60 MeV for several nuclides.

In this Letter we report measurements of σ_R for 60-MeV protons for ten targets: ^{12}C , ^{27}Al , ^{56}Fe , ^{58}Ni , ^{59}Co , ^{60}Ni , ^{68}Zn , ^{90}Zr , ^{120}Sn , and ^{208}Pb . All targets were enriched to at least 90% and they were about 150 to 200 keV thick, except the carbon which was 400 keV thick.

The method for measuring proton total reaction cross sections in this energy range was first reported by Gooding.⁴ It works as follows. A monoenergetic, collimated beam of protons, free of contamination by other particles, passes through a system of thin plastic scintillators, then through a target, and finally stops in a thick scintillator, subtending a substantial solid angle from the target. To a first approximation the number of events in which there is a proton in the passing counters in anticoincidence with the stopping counter is proportional to σ_R . To take account of the nuclear reactions in the stopping counter and several other effects, the measurement is repeated for the same number of incident protons

but with the target removed and the beam energy reduced by an amount equal to the energy loss in the target. This method is handicapped by the large number of reactions in the thick stopping counter relative to the number of reactions in the target. It is also limited in counting rate since the thick counter can accept only about 5×10^3 protons/sec before its response begins to deteriorate on account of gain shifts. We use an improved method recently reported by Dicello, Igo, and Roush.⁵ It is illustrated schematically in Fig. 1. The passing counters 1 and 2 are in coincidence while the annular counter 3 vetoes protons scattered by 1 and 2. The event $12\bar{3}$ defines a proton going into the target. In this notation unbarred numbers mean the counters are in coincidence, barred numbers in anticoincidence. Protons passing through the target are detected by a thin plastic scintillator 4 which subtends $\pm 13^\circ$ at the target. Protons scattered by the target through an angle $13^\circ < \theta < 45^\circ$ are detected by a thick plastic scintillator 5. This arrangement has the advantage over the original method that nearly all protons pass through counter 4 and are stopped by a nickel button behind it. Since counter 4 is thin, the pulse height is small and in addition only few nuclear reactions occur in it. The thick counter 5 now counts relatively slowly and poses no limit to the rate. The combination

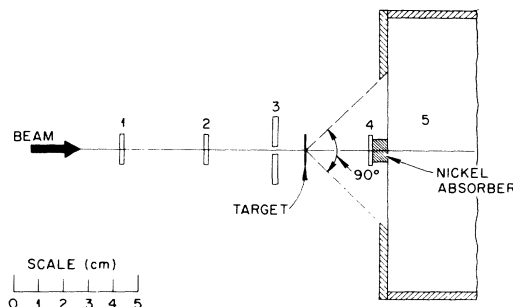


FIG. 1. Schematic layout of the detectors. Only the distances between the counters are to scale.

of these two effects allows us to work with $(5 \text{ to } 7) \times 10^4$ protons/sec. In fact, our equipment performed satisfactorily at rates up to 2×10^5 protons/sec, but we ran at the lower rates to avoid any difficulties that might be caused by changes of beam intensity.

For this experiment we used protons from the Oak Ridge isochronous cyclotron. After passing through counters 1 and 2 the energy was about 60 MeV at the target. The energy spread of the beam was ± 150 keV, and the beam spot at the tar-

get was circular, 2.5 mm in diameter. Standard fast modular electronics were used throughout; the resolving time plus dead time was usually around 30 nsec. The beam bursts of the cyclotron were separated by 45 nsec and random coincidences were thus eliminated. Target-in and target-out measurements were made and because of the small number of nuclear reactions in counter 4, a typical measurement in σ_R , to an accuracy of $\pm 3\%$ for one target, took about 45 min.

To obtain σ_R we use the formula

$$\Sigma = \frac{1}{n} \left\{ \frac{[(12\bar{3}\bar{4})_{\text{in}} - (12\bar{3}\bar{4})_{\text{out}}] - [(12\bar{3}\bar{4}\bar{5})_{\text{in}} - (12\bar{3}\bar{4}\bar{5})_{\text{out}}]}{12\bar{3}} \right\} (1+k)$$

where $\Sigma = \sigma_R + \sigma_{\text{el}}(\theta > 45^\circ) - \sigma_{\text{inel}}(\theta < 45^\circ)$, n is the number of atoms per cm^2 in the target, and k is the probability that a proton will escape detection by reacting in counter 5 and is obtained from Measday.⁶ The subscripts "in" or "out" are for target-in and target-out runs.

The events from counter 5 gated by $12\bar{3}\bar{4}$ were stored in a multichannel analyzer. The value of $12\bar{3}\bar{4}\bar{5}$ is obtained by integrating the proton spectrum down to an energy 6 MeV below the elastic peak. Both $\sigma_{\text{el}}(\theta > 45^\circ)$ and $\sigma_{\text{inel}}(\theta < 45^\circ)$ are small and are taken from published work where it exists. Where these cross sections are poorly known the error introduced is not large since typical values of $\sigma_{\text{el}}(\theta > 45^\circ)$ and $\sigma_{\text{inel}}(\theta < 45^\circ)$ are about 3% of σ_R . To calculate σ_R from our experiment we assume that the total reaction cross section leading to charged particles for $\theta < 13^\circ$ can be neglected because the cross section does not exceed a few millibarns in this solid angle.

To check our equipment we made some measurements at 30 MeV and our results are in good agreement with previous work.⁷⁻⁹ A full report of all our measurements of σ_R from 30 to 60 MeV together with an optical-model analysis will be published elsewhere.

The results of our 60-MeV measurements are given in Table I and are shown as a function of $A^{2/3}$ in Fig. 2. Also shown in Fig. 2 are the previous measurements of Meyer, Eisberg, and Carlson² as well as the 55-MeV neutron reaction cross-section measurements.³ Our results disagree with those of Meyer, Eisberg, and Carlson.² In their experiment the targets were 9 MeV thick; therefore, a 9-MeV absorber had to be used in the target-out measurements to eliminate the effect of reactions in the stopping counter.

However, this scheme introduces effects due to the difference in the elastic scattering cross section from the slits and the beam counters themselves at the two energies. In addition, the thick absorber increased the angular divergence of the beam at the beam counters. Both these phenomena tend to lower the measured reaction cross section, and our estimates indicate that they account for the difference between our results and

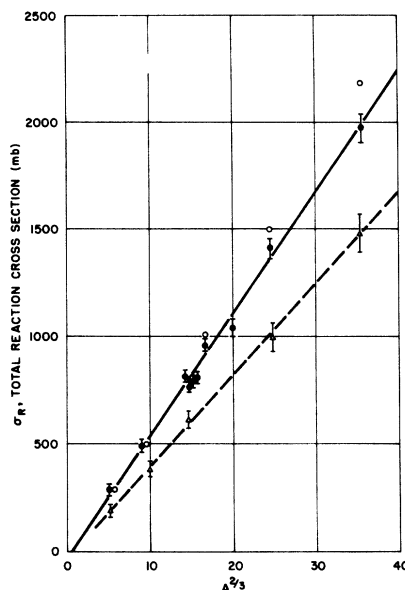


FIG. 2. The proton reaction cross section at 60 MeV vs $A^{2/3}$. The full circles are our data. The open circles are the 55-MeV neutron reaction cross sections of Voss and Wilson. The triangles correspond to the 60-MeV proton reaction cross-section measurements of Meyer, Eisberg, and Carlson. The straight lines are fits to the data.

Table I. Experimental results and optical model parameters obtained from a fixed-geometry search. For these searches the fixed parameters were $r_0 = 1.16$ F, $a = 0.75$ F, $r_0' = 1.37$ F, $a' = 0.63$ F, $V_S = 6.04$ MeV, $r_S = 1.064$ F, and $a_S = 0.738$ F. V , W , and W_D are, respectively, the central part of the real potential, the imaginary volume, and the imaginary surface part of the potential.

Target	V (MeV)	W (MeV)	W_D (MeV)	σ_R (calculated) (mb)	σ_R (experimental) (mb)
^{12}C	34.05	7.12	0.06	287	293 ± 12
^{27}Al	37.27	7.25	0.12	510	491 ± 26
^{56}Fe				a	808 ± 28
^{58}Ni	39.61	7.01	0.50	880	750 ± 25
^{60}Ni				a	796 ± 27
^{59}Co				a	777 ± 28
^{68}Zn	41.82	7.93	1.23	1103	940 ± 35
^{90}Zr	40.52	6.03	1.14	1177	1038 ± 32
^{120}Sn	44.76	7.03	1.99	1527	1453 ± 46
^{208}Pb	47.12	5.98	4.15	2136	1980 ± 90

^aNo analysis was made for the ^{56}Fe , ^{60}Ni , and ^{59}Co since there are no elastic-scattering data at 61.4 MeV.

the Minnesota measurements.² Furthermore we now find that there is no longer a glaring disagreement between neutron and proton reaction cross sections.

Our choice of targets was in part dictated by the fact that their elastic-scattering cross sections had been measured by Fulmer et al.¹ We then analyzed our results by fitting the elastic data as well as σ_R simultaneously with an optical model with fixed geometry. The model¹⁰ has been used successfully to fit the available scattering and polarization data from 30 to 60 MeV. Table I shows the results of this calculation as well as our experimental data. The value of χ^2 for this calculation is on the average about as large as it was for the elastic-scattering data alone, except for Zr where it is three times larger. We also note that V is about the same as it was on the basis of the elastic data alone; W is about 7 ± 1 MeV and not obviously correlated with A , while W_D shows an unmistakable A dependence, rising monotonically from 0.12 MeV for Al to 4.2 MeV for Pb. This kind of behavior of W and W_D was suspected previously at 30 MeV¹¹ and 40 MeV,¹⁰ but it becomes more explicit at 60 MeV with optical model searches influenced by reaction cross-section data.

It was originally hoped that measurements of

σ_R would produce information about the imaginary part of the optical model which cannot be obtained by investigating the elastic channels alone; this expectation appears to have been reasonable. However, as is evident from Table I, the measured reaction cross sections are 5-15% smaller than the calculations based on the average-geometry optical model.¹⁰ This systematic discrepancy strongly suggests to us that a revision is necessary in the average-geometry parameters to represent properly reaction cross sections as well as elastic scattering and polarizations.

The authors wish to thank C. N. Waddell for some illuminating discussions before these measurements were started. We are grateful to R. W. Rutkowski and W. J. Roberts for their help in taking data, to the cyclotron operators for providing the unusual low-intensity beams, and to M. E. Wimberley for the artful construction of the mechanical equipment. One of us (J.J.H.M.) wishes to thank the Centre National de la Recherche Scientifique and NATO for their financial support, and the Oak Ridge National Laboratory for its generous hospitality.

*Research sponsored by the U. S. Atomic Energy

Commission under contract with Union Carbide Corporation.

†NATO Fellow; on leave from Institut des Sciences Nucléaires, Cyclotron, Grenoble, France.

¹C. B. Fulmer, J. B. Ball, A. Scott, and M. L. Whiten, *Phys. Letters* **24B**, 505 (1967), and *Phys. Rev.* (to be published).

²V. Meyer, R. M. Eisberg, and R. F. Carlson, *Phys. Rev.* **117**, 1334 (1960).

³R. Voss and R. Wilson, *Proc. Roy. Soc. (London)*, Ser. A **236**, 41 (1958).

⁴T. J. Gooding, *Nucl. Phys.* **12**, 24 (1959).

⁵J. F. Dicello, G. J. Igo, and M. L. Roush, *Phys. Rev.* **157**, 1001 (1967).

⁶D. F. Measday, *Nucl. Instr. Methods* **34**, 353 (1965).

⁷M. Q. Makino, C. N. Waddell, and R. M. Eisberg, *Nucl. Phys.* **50**, 145 (1964).

⁸J. F. Turner, B. W. Ridley, P. E. Cavanagh, G. A. Gard, and A. G. Hardacre, *Nucl. Phys.* **58**, 509 (1964).

⁹M. Q. Makino, C. N. Waddell, R. M. Eisberg, and J. Hestenes, *Phys. Letters* **9**, 178 (1964).

¹⁰M. P. Fricke, E. E. Gross, B. J. Morton, and A. Zucker, *Phys. Rev.* **156**, 1207 (1967).

¹¹G. R. Satchler, *Nucl. Phys.* **A92**, 273 (1967).

PHOTOPRODUCTION OF $K^+\Lambda$ AND $K^+\Sigma^0$ FROM HYDROGEN FROM 5 TO 16 GeV*

A. M. Boyarski, F. Bulos, W. Busza, R. Diebold, S. D. Ecklund, G. E. Fischer, Y. Murata,†
J. R. Rees, B. Richter, and W. S. C. Williams‡

Stanford Linear Accelerator Center, Stanford University, Stanford, California 94305

(Received 1 April 1969)

Cross sections for the reactions $\gamma p \rightarrow K^+\Lambda$ and $\gamma p \rightarrow K^+\Sigma^0$ have been measured at squared four-momentum transfer ($-t$) from 0.005 to 2 GeV², at photon energies 5, 8, 11, and 16 GeV. For $-t > 0.2$ GeV² each of the K^+ cross sections is about $\frac{1}{3}$ of the π^+n photoproduction cross section, having nearly the same energy and momentum-transfer dependence. The K^+ cross sections fall off at small $|t|$, however, in contrast to the sharp forward spike seen in π^+n ; this leads to a disagreement with an SU(3) prediction for $-t < 0.1$ GeV². The ratio of $K^+\Sigma^0$ to $K^+\Lambda$ cross sections is typically between 0.5 and 1.0.

Cross sections for the reactions $\gamma p \rightarrow K^+\Lambda$ and $\gamma p \rightarrow K^+\Sigma^0$ were measured simultaneously with $\gamma p \rightarrow \pi^+n$ using the Stanford Linear Accelerator Center 20-GeV magnetic spectrometer.¹ This extends work done previously at other laboratories in the few GeV range.²⁻⁵ The experimental apparatus has been described previously.⁶

The measured K^+ yields were corrected for K^+ decay; detection inefficiencies in the shower counter, range hodoscope, and Čerenkov counters; absorption in detectors; dead time and accidental coincidences; and empty-target yields. The errors given in the figures reflect only the counting statistics folded with a 5% error to account for fluctuating systematics. In addition, there is an overall uncertainty in normalization of $\pm 10\%$.

Cross sections were obtained by measuring K^+ yields produced by photons near the end point of the bremsstrahlung spectrum. For each event, a missing mass was calculated for a photon energy equal to the bremsstrahlung end-point energy. The yield as a function of missing mass then has a step at the Λ mass plus a second step, beginning at the Σ^0 mass. The shape of the steps is a

reflection of the bremsstrahlung spectrum⁷ and the variation of the cross section with energy, folded with the finite experimental resolution. The resolution was accurately determined from the step in the π^+n reaction measured at the same time; it was typically 0.04 GeV² (standard deviation), in units of missing-mass squared, compared with a separation of 0.18 GeV² between the Λ and Σ^0 steps. The position of the Λ and Σ^0 steps was computed from the measured position of the π^+n step which agreed with the position expected from the calibration of the beam and spectrometer momenta to better than 0.3%. The cross sections were obtained by least-squares fitting the height of the Λ and Σ^0 steps. To represent background processes a polynomial in missing-mass squared was included beginning at the threshold for $\gamma p \rightarrow K^+\Lambda\pi^0$.

The results of the cross-section measurements are given in Figs. 1 and 2. Both K reactions fall exponentially for $-t > 0.5$ GeV² approximately as $e^{(3.0 \pm 0.2)t}$, similar to the $\gamma p \rightarrow \pi^+n$ cross sections. At smaller $|t|$, the K^+ cross sections become flat in t and then decrease as $-t$ goes towards zero, markedly different from π^+n ,